Bell, J. E., Beyer, T. A., & Hill, R. L. (1976) *J. Biol. Chem. 251*, 3003.
Beyer, T. A., Sadler, J. E., & Hill, R. L. (1980) *J. Biol. Chem. 255*, 2364.
Bohlen, P., Stein, S., Dairman, W., & Udenfriend, S. (1973) *Arch. Biochem. Biophys. 155*, 213.
Chiang, C. K., McAndrew, M., & Barker, R. (1979) *Carbohydr. Res. 70*, 93.
Cuatrecasas, P. J. (1970) *J. Biol. Chem. 245*, 3059.
Dorman, D. E., & Roberts, J. D. (1970) *J. Am. Chem. Soc. 92*, 1355.
Excoffier, G., Gagnaire, D. Y., & Taravel, F. R. (1977) *Carbohydr. Res. 56*, 229.
Gagnaire, D. Y., Taravel, E. R., & Vignon, M. R. (1977) *Nouv. J. Chim. 1*, 423.
Hamer, G. K., Balza, F., Cyr, N., & Perlin, A. S. (1978) *Can. J. Chem. 56*, 3109.
Hirotsu, K., & Shimada, A. (1974) *Bull. Chem. Soc. Jpn. 47*, 1872.
Inch, T. D. (1972) *Annu. Rep. NMR Spectrosc. 5A*, 305.
Jacquinet, J. C., & Sinay, P. (1976) *Tetrahedron 32*, 1693.
Jacquinet, J. C., & Sinay, P. (1977) *J. Org. Chem. 42*, 720.
Lemieux, R. U., & Koto, S. (1974) *Tetrahedron 30*, 1933.
Lemieux, R. U., & Driguez, H. (1975) *J. Am. Chem. Soc. 97*, 4063.
Lemieux, R. U., Koto, S., & Voisin, D. (1979) in *Anomeric Effect Origin and Consequences* (Szarek, W. A., & Horton, D., Eds.) Adv. Chem. Ser. No. 87, p 17, American Chemical Society, Washington, D.C.
Lemieux, R. U., Bock, K., Delbaere, L. T. J., Koto, S., & Rao, V. S. (1980) *Can. J. Chem. 58*, 631.
Moffat, J. G. (1966) *Methods Enzymol. 8*, 136.
Naoi, M., & Lee, Y. C. (1974) *Anal. Biochem. 57*, 640.
Nunez, H. A., & Barker, R. (1976) *Biochemistry 15*, 3843.
Nunez, H. A., & Barker, R. (1979) *Fed. Proc., Fed. Am. Soc. Exp. Biol. 38*, 991.
Nunez, H. A., & Barker, R. (1980) *Biochemistry 19*, 489.
Nunez, H. A., O'Connor, J., Rosevear, P. R., & Barker, R. (1981) *Can. J. Chem. 59*, 2086.
Rosevear, P. R., Nunez, H. A., & Barker, R. (1980) *Fed. Proc., Fed. Am. Soc. Exp. Biol. 39*, 2506.
Sadler, J. E., Rearick, J. I., Paulson, J. L., & Hill, R. L. (1979) *J. Biol. Chem. 254*, 4434.
Serianni, A. S., Nunez, H. A., & Barker, R. (1979a) *Carbohydr. Res. 72*, 71.
Serianni, A. S., Clark, E. L., & Barker, R. (1979b) *Carbohydr. Res. 72*, 79.
Walker, T. E., London, R. E., Whaley, T. W., Barker, R., & Matwiyoff, N. A. (1976) *J. Am. Chem. Soc. 98*, 5807.

Single-Crystal Electron Paramagnetic Resonance Studies of Photolyzed Oxy- and Nitric Oxide–Cobalt Myoglobins†

Hiroshi Hori, Masao Ikeda-Saito,* John S. Leigh, Jr., and Takashi Yonetani

ABSTRACT: Low-temperature photodissociation of oxygen from oxy–cobalt myoglobin was studied by single-crystal electron paramagnetic resonance (EPR) spectroscopy at 5 K. The photolyzed oxy–cobalt myoglobin exhibited an EPR spectrum consisting of two nonequivalent sets (species I and II) of the principal values and eigenvectors of the g tensors: $g_1^{I} = 3.55$, $g_2^{I} = 3.47$, and $g_3^{I} = 2.26$ for species I, and $g_1^{II} = 2.04$, $g_2^{II} = 1.93$, and $g_3^{II} = 1.86$ for species II, which resembled neither the deoxy nor the oxy form. Possible models of the photodissociated state of oxy–cobalt myoglobin are proposed by comparison with cobalt porphyrin complexes. The photolyzed product of nitric oxide–cobalt myoglobin exhibited new EPR signals at $g = 4.3$ and a very broad signal at around $g = 2$. The principal g values have been determined from the single-crystal EPR measurements: $g_1 = 4.39$, $g_2 = 4.27$, and $g_3 = 4.00$. Analysis of another EPR signal around $g = 2$ was difficult due to its broadness. Magnetic interactions were observed. An isotropic EPR signal at $g = 4.3$ suggested a weakly spin-coupled system between cobaltous spin ($S = {}^1/_2$ or ${}^3/_2$) and nitric oxide spin ($S = {}^1/_2$).

The light-induced dissociations of ligands such as oxygen (O_2), carbon monoxide (CO), and nitric oxide (NO) from myoglobin (Mb),[1] hemoglobin (Hb), and other hemoproteins are well-known. The elucidation of the electronic and stereochemical natures of these photolyzed products has an important implication in our understanding of the molecular mechanisms of ligand binding and photolysis.

Artificial myoglobins and hemoglobins substituted with cobaltous protoporphyrin IX for protoheme are capable of reversible oxygenation (Hoffman & Petering, 1970; Yonetani et al., 1974a). As previously demonstrated, oxy–CoMb and oxy–CoHb are readily photolyzed at liquid helium temperature (4.2 K). The optical absorption spectra of the photolyzed products are indistinguishable from those of the corresponding deoxy compounds. However, the photolyzed product exhibits new EPR extrema at $g = 3.87$ and around $g = 1.9$, which resemble neither the deoxy nor the oxy form, suggesting the possibility that the photolyzed product may be in a new

† From the Department of Biochemistry and Biophysics, University of Pennsylvania School of Medicine, Philadelphia, Pennsylvania 19104 (H.H., M.I.-S., J.S.L., and T.Y.), the Department of Biophysical Engineering, Faculty of Engineering Science, Osaka University, Toyonaka, Osaka 560, Japan (H.H.), and the Institut National de la Santé et de la Recherche Médicale, Laboratory Unit 128, Montpellier 34033, France (T.Y.). *Received July 14, 1981.* This investigation was supported by National Institutes of Health Grants HL 14508 (T.Y.), GM 12202 (J.S.L.), and GM 25052 (J.S.L.) and by National Science Foundation Grant PCM 79-22841 (T.Y.). This is paper 16 in the series on cobalt myoglobins and hemoglobins.

[1] Abbreviations: Mb, myoglobin; Hb, hemoglobin; EPR, electron paramagnetic resonance; Co^{II}TpivPP, cobalt(II) *meso*-tetrakis($\alpha,\alpha,\alpha,\alpha$-*o*-pivalamidophenyl)porphyrin.

0006-2960/82/0421-1431$01.25/0

electronic state containing a high-spin Co(II) ion ($3d^7$, $S = {}^3/_2$) (Yonetani et al., 1974b). The photolyzed form is found to be stable below 10 K, and recombination of the dissociated O_2 occurs only at higher temperatures. The processes of photodissociation and thermal recombination have been examined, and the activation energy of recombination has been estimated to be 570 cal/mol of CoMb (Iizuka et al., 1974). On the contrary, the photolyzed form of oxy–CoHb (*Glycera*), in which the distal histidine of Mb is replaced by a leucyl residue (Padlan & Love, 1974), exhibits the same optical and EPR spectra as those of the deoxy form (Ikeda-Saito et al., 1977). This difference between CoMb and CoHb (*Glycera*) has been interpreted in relation to the possible role of the distal histidine in oxygen binding in CoMb (Ikeda-Saito et al., 1977).

From these results, several models of the photolyzed form have been demonstrated. However, none of these models have been able to sufficiently explain both the EPR and optical absorption spectra of the photolyzed product (Yonetani et al., 1974b; Iizuka et al., 1974; Ikeda-Saito et al., 1977). In this paper, we will propose a new model for these photolyzed products from the single-crystal EPR analyses of photolyzed oxy–CoMb and nitric oxide–CoMb.

Experimental Procedures

Oxy–CoMb was prepared by recombination of globin from sperm whale myoglobin and cobaltous protoporphyrin IX, followed by CM-cellulose column chromatography according to the method of Yonetani et al. (1974a). Oxy-CoMb crystals were grown in an ammonium sulfate–phosphate solution at pH 6.1 (Petsko et al., 1978). The deoxy–CoMb single crystals were prepared directly from the oxy–CoMb crystals by anaerobic addition of sodium dithionite. The nitric oxide–CoMb crystals were prepared as follows: after nitrogen gas was gently bubbled into the mother liquid containing oxy–CoMb crystals for several minutes, a small amount of sodium nitrite ($NaNO_2$) was anaerobically added into the mother liquid, followed by a small amount of solid sodium dithionite. In these crystals (so-called type A crystals, with a space group of $P2_1$ and a Z value of 2 molecules/unit cell) (Kendrew & Parrish, 1956; Petsko et al., 1978), the three crystallographic axes (a, b, and c^*) are readily identified by visual examination, where c^* is perpendicular to a and b by definition.

Whole blood of *Glycera dibranchiata* was a gift of Dr. E. A. Padlan of the National Institutes of Health, Bethesda, MD. CoHb (*Glycera*) was reconstituted and purified as described elsewhere (Ikeda-Saito et al., 1977).

Cobalt(II) *meso*-tetrakis($\alpha,\alpha,\alpha,\alpha$-*o*-pivalamidophenyl)-porphyrin (Co^{II}TpivPP) was synthesized according to the method of Collman et al. (1974, 1978). A fluid solution of Co^{II}TpivPP was prepared directly by dissolving the above crystalline complex into toluene.

EPR measurements were carried out with S- (Micro Now Instruments Co., microwave bridge 802B and Varian console V-4502), X- (Varian E-109), and Q-band (Varian V-4503) EPR spectrometers with 100-kHz field modulation, which were operated at microwave frequencies of 3.79, 9.232, and 35.42 GHz, respectively.

EPR measurements for the single crystals were performed with an X-band spectrometer, interfaced with a PDP 11/40 computer system for data acquisition and analysis. The single crystals were mounted with a small quantity of grease on a quartz sample holder and held in an Air Products cryostat (LTD-3-110) for 5 K measurements. The holder mounted with the crystal was rotated manually in 5° or 10° steps. The EPR data of the resonance positions vs. the angles of rotation were least-squares fitted to Schonland's equation (Schonland, 1959) to determine the angular dependence of the square of the g values (g^2) by the PDP 11/40 computer. The principal values and the eigenvectors, with respect to the crystallographic axes, were determined according to Schonland's method.

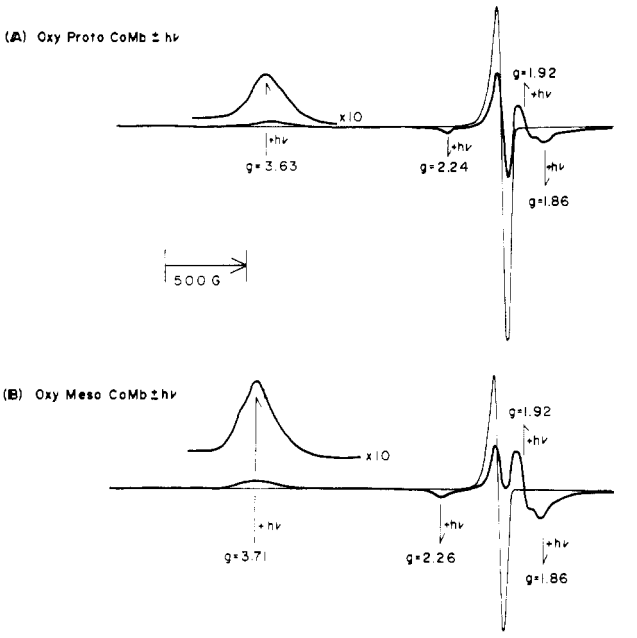

FIGURE 1: X-band spectra of photolyzed oxy–Co-protoMb (A) and oxy–Co-mesoMb (B) at 5 K. The EPR spectra of oxy–CoMbs are shown by the thin line. Spectra are recorded at 50 mW, and the field modulation is 5 G. Solution conditions are 0.1 M phosphate buffer, pH 7.

Low-temperature spectrophotometric measurements were carried out with a dual-beam spectrophotometer equipped with a double Dewar flask for liquid helium studies, which was constructed at the Johnson Foundation, University of Pennsylvania (Iizuka et al., 1974). The photolysis experiments were performed by illuminating the spectrophotometric and EPR samples with unfiltered tungsten light (Labsource, OH-150SR) at cryogenic temperature (~5 K).

Results

Photolyzed Products of the Oxy Complexes. Figure 1 illustrates the changes in the X-band powder EPR spectra of oxy–Co-protoMb and oxy–Co-mesoMb. The g values of the photolyzed products are different between Co-protoMb and Co-mesoMb. The g values of the photolyzed products of oxy–Co-mesoMb (g = 3.71 and around 1.9) are somewhat different from those reported previously (Yonetani et al., 1974b). The powder EPR spectrum of the photolyzed product of oxy–Co-protoHb (*Glycera*) was, on the other hand, identical with that of the deoxy form as reported previously (Ikeda-Saito et al., 1977), and not shown in Figure 1. The EPR spectra of the photolyzed product of oxy–CoMb were also recorded at S and Q bands and are illustrated in Figure 2, together with that at the X band and those of the deoxy forms. Though the Q-band spectra of deoxy–CoMb and oxy–CoMb were readily distorted at high microwave power with 100-kHz field modulation at 5 K, the line shape of the photolyzed product (g = 3.45) was very similar to that of the X-band spectrum. No hyperfine structure due to the ^{59}Co nucleus was observed. The g values were somewhat different from those of the S or the X band. We observed the small EPR signal of the deoxy form at g = 2.33 in the photolyzed oxy–CoMb at the S and Q bands.

The angular variations of the g^2 values for the photolyzed products of oxy–CoMb single crystals are shown in Figure 3. Two nonequivalent sets of the principal values for the g tensors

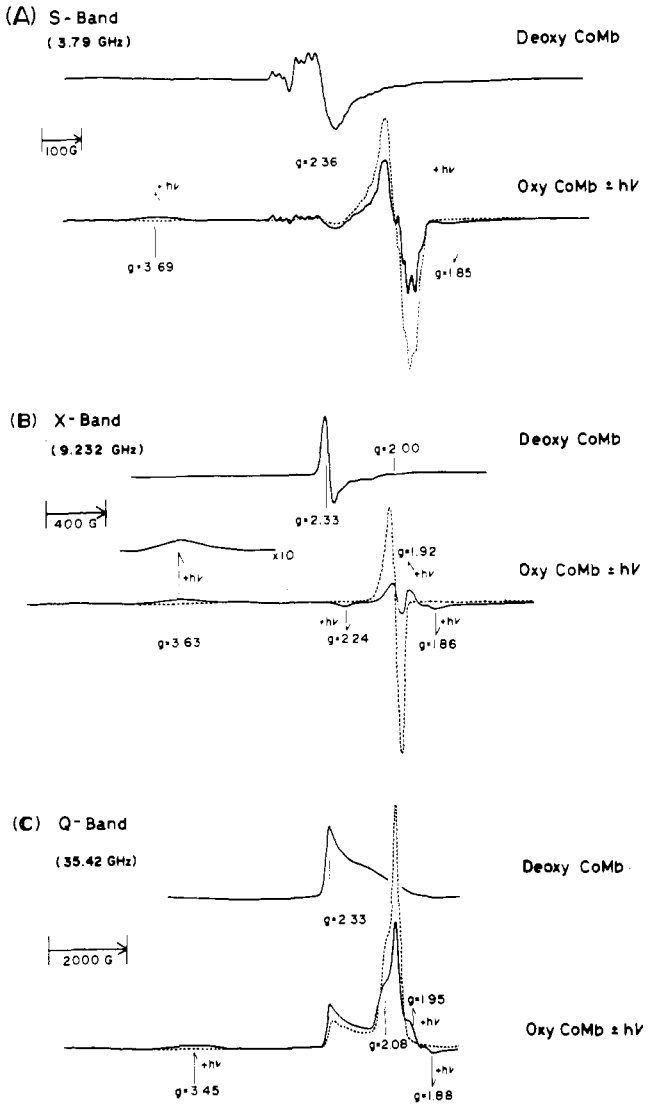

FIGURE 2: EPR spectra of deoxy–CoMb and the photolyzed product of oxy–CoMb at the S band (A), X band (B), and Q band (C). The dotted lines show the EPR spectra of oxy–CoMb before illumination. These spectra are recorded with high microwave power at 5 K.

and eigenvectors were found (species I and II). This was clearly shown in the *ac** and *bc** planes. In the *ab* plane, only one resonance was observed for species I, because the maximal g^2 value in this plane was located in the vicinity of the *a* axis. We failed to measure the EPR signal for species II in this plane, because the EPR signals from the remaining oxy form overlap the signals of species II. However, one of the principal *g* values ($g = 1.93$) for species II, which was assumed from the powder EPR spectrum shown in Figure 1, was located in the vicinity of the *c* crystalline axis and has a very strong signal intensity. Thus, we could approximately determine the *g* tensors and the eigenvectors for species II.

The principal *g* values are determined to be the following: $g_1^{I} = 3.55$, $g_2^{I} = 3.47$, and $g_3^{I} = 2.26$ for species I, and $g_1^{II} = 2.04$, $g_2^{II} = 1.93$, and $g_3^{II} = 1.86$ for species II, respectively. No hyperfine structure was observed in these EPR signals. In Figure 4, these principal axes are shown on the stereographic diagram. The direction of the minimal *g* value for species I ($g_3^{I} = 2.26$) is nearly parallel to the porphyrin plane. The experimental errors of *g* values and of the principal axis directions were ±0.01 and ±5°, respectively.

Photolyzed Products of the Nitric Oxide Complexes. Optical absorption spectra of nitric oxide–CoMb and nitric oxide–CoHb (*Glycera*) were changed to those of the corre-

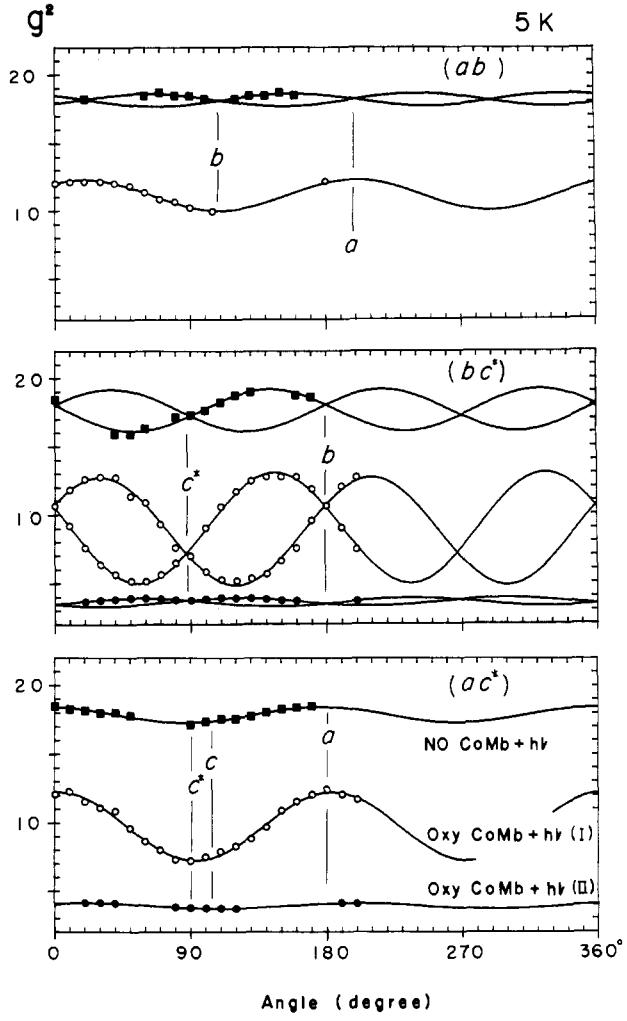

FIGURE 3: Angular variations of g^2 values of photolyzed nitric oxide–CoMb (■) and photolyzed oxy–CoMb species I (○) and II (●).

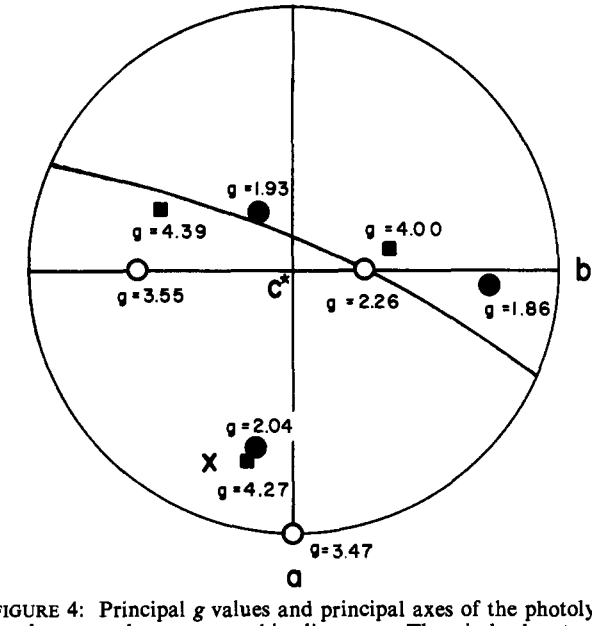

FIGURE 4: Principal *g* values and principal axes of the photolyzed products on the stereographic diagram. The circle denotes the porphyrin plane of deoxy–CoMb: (■) photolyzed nitric oxide–CoMb; (○) photolyzed oxy–CoMb (species I); (●) photolyzed oxy–CoMb (species II); (×) the direction of $g_{\parallel}$ which is prependicular to the porphyrin plane of deoxy–CoMb. These principal axes belong to site A CoMb molecules in the unit cell of the crystal. Another set of the principal axes belongs to site B and can be shown by symmetrical operation of a single crystal (the *b* axis: dyad axis) and thus is not shown in this diagram.

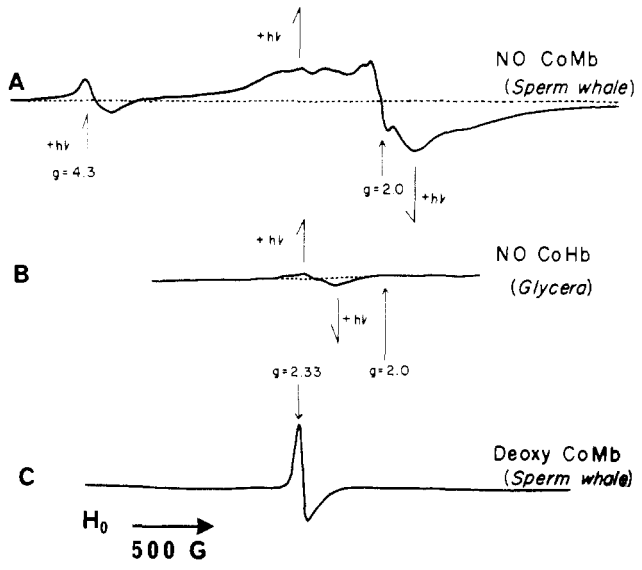

FIGURE 5: X-band spectra of photolyzed nitric oxide–Co-protoMb (A), deoxy–Co-protoMb (C) (sperm whale), and nitric oxide–Co-protoHb (*Glycera*) (B) at 5 K. The EPR spectra shown by the dotted line are nitric oxide complexes. Spectra are recorded at 10 mW, and the field modulation is 5 G. Solution conditions are 0.1 M phosphate buffer, pH 7.

sponding deoxy form upon illumination of 4.2 K. Nitric oxide complexes of CoMb and CoHb (*Glycera*) exhibited no EPR absorption due to spin pairing (Yonetani et al., 1972). The photolyzed product of nitric oxide–CoMb exhibited a relatively narrow EPR signal at $g = 4.3$ (peak to peak width in the first derivative spectrum: $\Delta H = 160$ G) and a broad signal around $g = 2$ ($\Delta H \sim 800$ G) as shown in Figure 5A. On the other hand, the photolyzed product of nitric oxide–CoHb (*Glycera*) exhibited a broad EPR signal around $g = 2.33$, which is different from that of the deoxy form (Figure 5B). The EPR spectra of photolyzed products of oxy- and nitric oxide–CoMbs were recorded at several microwave power ranges, from 10 μW to 100 mW. However, no hyperfine structure due to the ^{59}Co nucleus with $I = {}^7/_2$ was observed in these EPR spectra. The reversion of the photolyzed products to the original nitric oxide state was retarded below ~20 K.

The angular variations of the g^2 values for the photolyzed products of nitric oxide–CoMb single crystals, as shown in Figure 3, indicate that the g tensor is nearly isotropic at $g = 4.3$. The principal g values were determined to be the following: $g_1^{NO} = 4.39$, $g_2^{NO} = 4.27$, and $g_3^{NO} = 4.00$. We were unable to analyze the broad EPR signal around $g = 2$ because of its low signal intensity. These principal g values and eigenvectors are summarized in Table I and are shown on the stereographic diagram of Figure 4. The experimental accuracies of the g values and of the principal axis directions were ±0.02 and ±5°, respectively.

Model Cobalt Complexes. Figure 6 illustrates the optical absorption spectra of Co^{II}TpivPP complexes at 77 K in the visible region. The optical absorption spectrum of tetracoordinated Co^{II}TpivPP in toluene was found to be very similar to that of pentacoordinated Co^{II}TpivPP·2-methylimidazole, exhibiting an absorption peak around 530 nm with a shoulder around 535 nm. On the other hand, the optical absorption spectrum of hexacoordinated oxy–Co^{II}TpivPP·2-methylimidazole shows quite a different spectrum, exhibiting an absorption peak at 560 nm.

Figure 7 illustrates the EPR spectra of square-planar tetracoordinated Co^{II}TpivPP (A), pentacoordinated Co^{II}TpivPP·2-methylimidazole (B), pentacoordinated oxy–Co^{II}TpivPP (C), and hexacoordinated oxy–Co^{II}TpivPP·2-methylimidazole (D) in toluene at 77 K, respectively. The g values and hyperfine coupling constants of tetracoordinated Co^{II}T-

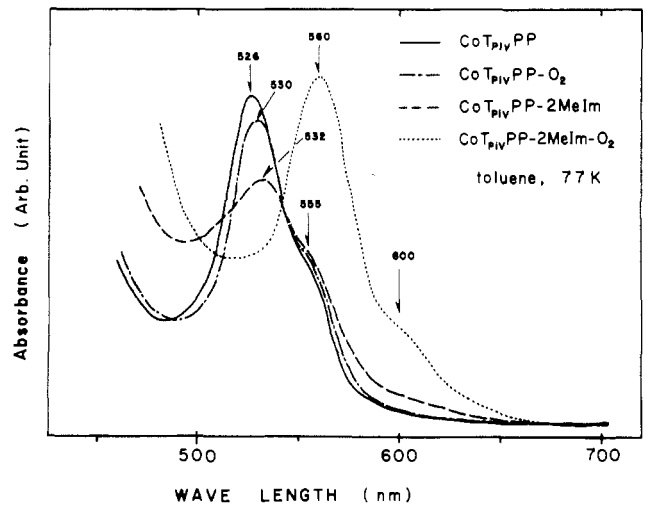

FIGURE 6: Optical absorption spectra of Co^{II}TpivPP complexes in toluene at 77 K (visible region).

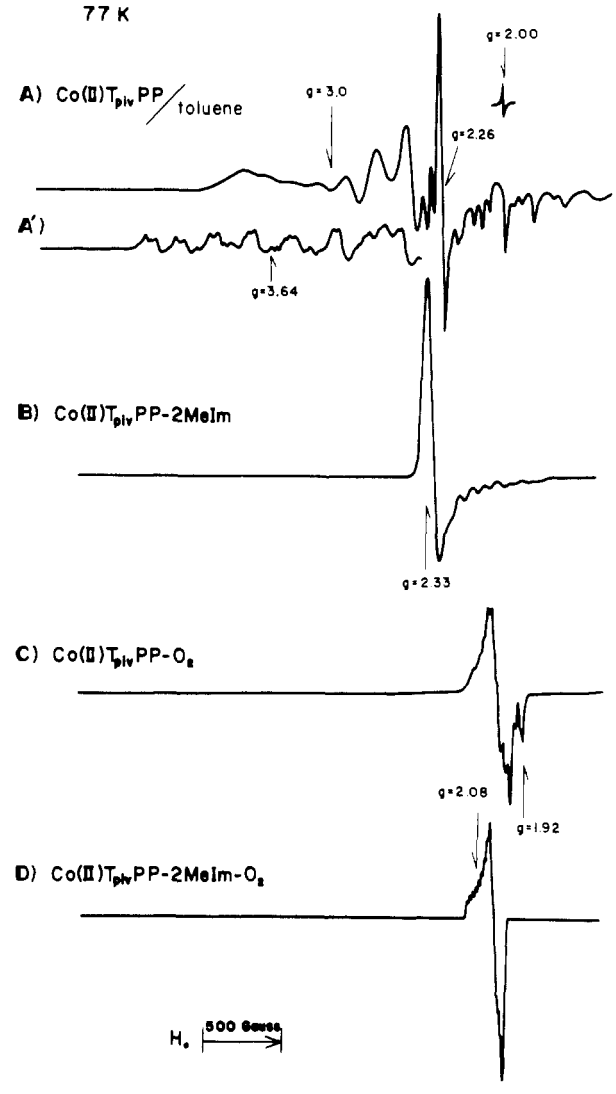

FIGURE 7: X-band EPR spectra of Co^{II}TpivPP complexes in toluene at 77 K: tetracoordinated complex (A and A'); pentacoordinated complex—deoxy–Co^{II}TpivPP·2-methylimidazole (B); oxy–Co^{II}TpivPP (C); hexacoordinated oxy–Co^{II}TpivPP·2-methylimidazole (D). The spectra in A and A' are recorded under different freezing conditions, in glassy frozen toluene (A) and in cracked frozen toluene (A').

Table I: Principal g Values and Directions in a Single Crystal

complex	temp (K)	principal g values	angle (deg) to a	b	c^*
O_2-CoMb + $h\nu$ (I)	5	$g_1 = 3.55$	90	−30	60
		$g_2 = 3.47$	0	90	90
		$g_3 = 2.26$	90	60	30
O_2-CoMb + $h\nu$ (II)	5	$g_1 = 2.04$	23	−79	70
		$g_2 = 1.93$	−67	−76	27
		$g_3 = 1.86$	85	18	73
NO-CoMb + $h\nu$ (I)	5	$g_1 = 4.39$	−70	−41	57
		$g_2 = 4.27$	22	−78	72
		$g_3 = 4.00$	−83	52	39
NO-CoMb + $h\nu$ (II)	5	undetermined			
deoxy-CoMb	77	$g_1 = 2.328$ ($g_\perp$)	−66	−63	38
		$g_2 = 2.322$ ($g_\perp$)	79	37	55
		$g_3 = 2.044$ ($g_\parallel$)	27	−68	76

pivPP changed drastically under different freezing conditions (Figure 7A,A′) as pointed out by Walker (1970).

The photolysis of the oxy-Co^{II}TpivPP·2-methylimidazole complex was performed in frozen toluene at 5 K. The photodissociation could be observed in the EPR measurement for the first time. The EPR spectrum of the photolyzed product (figure not shown) was that of the deoxy form. The signal intensity of the photolyzed product was very low as compared with that of the remaining unphotolyzed oxy-Co^{II}TpivPP·2-methylimidazole complex. Thus, we could not detect the photolyzed product in the optical absorption spectrum at 4.2 K.

Deoxy States. Deoxy-CoMb exhibited an EPR absorption of axial symmetry, which is derived from Co(II) ($3d^7$, $S = {}^1/_2$), as previously reported (Hoffman & Petering, 1970; Chien & Dickinson, 1972; Yonetani et al., 1974b). The EPR spectra of deoxy-CoMb crystals at 77 K showed a well-resolved octuplet hyperfine structure due to the coupling of the unpaired electron to the ^{59}Co nucleus with $I = {}^7/_2$. Each of these hyperfine lines was further split into triplets by superhyperfine coupling with a ^{14}N nucleus of the proximal histidine residue. A maximal value of $A^{Co} = 77$ G was observed along the normal of the porphyrin plane. The hyperfine coupling was not resolved in the porphyrin plane, and the minimal line width of the EPR signal in this plane was estimated to be 35 G. The nitrogen superhyperfine splitting was observed to be 17 G with the magnetic field perpendicular to the porphyrin plane. From the analysis of the g tensor, the principal g values are $g_{xx} = 2.33$, $g_{yy} = 2.32$, and $g_{zz} = 2.04$, where z is along the normal of the porphyrin plane. The g tensor and hyperfine coupling tensor share the same principal axes. The present single-crystal results are in good agreement with those observed previously for powder samples (Hoffman & Petering, 1970; Yonetani et al., 1974b) and single crystals (Chien & Dickinson, 1972), and are listed in Table I. The experimental accuracies of g values and of the principal axis directions were ±0.01 and ±5°, respectively.

Discussion

Photolysis of Oxy-Cobalt Complexes. As previously demonstrated, the optical absorption spectra of photolyzed oxy-CoMb and oxy-CoHb are indistinguishable from those of the corresponding deoxy compounds, whereas their EPR spectra, having extrema at $g = 3.87$ and around $g = 1.9$, resemble the spectrum of neither the deoxy nor the oxy form (Yonetani et al., 1974b). The EPR signals at $g = 3.87$ and around $g = 1.9$ observed in photolyzed oxy-CoMb had been previously considered to derive from only one EPR species. However, our present single-crystal EPR study of photolyzed oxy-CoMb demonstrates that these EPR signals are composed of at least two distinct paramagnetic species. One species (species I) has a nearly axial symmetry ($g_1 = 3.55$, $g_2 = 3.47$, and $g_3 = 2.26$) with the direction of $g_3 = 2.26$ being nearly parallel to the porphyrin plane. The second EPR species (species II) has EPR signals around $g = 1.9$ ($g_1 = 2.04$, $g_2 = 1.93$, and $g_3 = 1.86$). These g values and the eigenvectors are quite different from those of the deoxy and oxy forms. The previous single-crystal data of oxy-CoMb at cryogenic temperature indicated that the bound oxygen molecule in oxy-CoMb assumes two distinct orientations (Chien & Dickinson, 1972; Dickinson & Chien, 1980; Hori et al., 1980). It would be resonable to assume that these orientations of the bound oxygen may be related to the two paramagnetic species which appear in the photolyzed products. An EPR study on CoHb (*Glycera*) has shown that the mode of interaction between the cobaltous ion and the proximal histidine is similar in deoxy-CoMb and in deoxy-CoHb (*Glycera*) and that the orientation of the bound oxygen molecule relative to the porphyrin plane in oxy-CoHb (*Glycera*) is somewhat different from that in oxy-CoMb, due to the difference in the environment of the distal site. The simple, well-resolved, hyperfine splitting observed in the oxy EPR spectra of CoHb (*Glycera*) (Ikeda-Saito et al., 1977) suggests the existence of only one EPR species at cryogenic temperature. The photolyzed form of CoHb (*Glycera*) exhibited EPR and optical spectra similar to those of the deoxy form (Ikeda-Saito et al., 1977). The photolyzed product of the oxy-Co^{II}TpivPP·2-methylimidazole complex, which may be employed as a model of oxy-CoHb (*Glycera*), exhibited the EPR signal of the deoxy form of Co^{II}TpivPP·2-methylimidazole in frozen toluene at 5 K. The EPR signals at $g = 3.87$ and around $g = 1.9$ were not observed in the the photolyzed product of oxy-Co^{II}TpivPP·2-methylimidazole.

Model of Photolyzed Oxy-CoMb. Before discussing the chemical nature of the photolyzed product of oxy-CoMb, let us consider the optical and EPR spectra of Co(II) model complexes, which closely resemble those of the photolyzed product. Two spin states are possible for the Co(II) ion: low-spin ($3d^7$, $S = {}^1/_2$) and high-spin ($3d^7$, $S = {}^3/_2$) states. Effective g values ranging from $g = 3$ to $g = 8$ have been reported for high-spin (Co(II) complexes (Goodman & Raynor, 1970), though the coordination structures of the complexes are not known. The majority of low-spin Co(II) complexes have an EPR absorption near the free spin value of $g \sim 2$ (Goodman & Raynor, 1970). EPR parameters for several tetracoordinated square-planar low-spin Co(II) complexes have been reported (Walker, 1970, 1974; Hoffman et al., 1973; Urbach et al., 1974; Chacko & Monoharan, 1974): complexes with symmetry of D_{2h} or less always have one g value ranging from $g = 2.6$ to $g = 3.8$ in the plane, with the other two g values near $g = 2.0$. Fantucci & Valenti (1976) have proposed on theoretical grounds that the unpaired electron in square-planar, low-spin complexes is located mainly in the d_{yz} cobalt orbital. The EPR spectra of tetracoordinated Co(II) complexes of tetrakis(*p*-methoxyphenyl)porphyrin have been reported to have the maximal g value, $g \sim 2.9$–3.2, with large hyperfine coupling (Walker, 1970). Walker has pointed out that these spectra are readily altered under different freezing conditions, indicating that the electronic state of the tetracoordinated Co(II) porphyrin may be highly sensitive to its environmental conditions, such as the type of solvent, and the deformation of the porphyrin. The EPR spectrum of tetracoordinated Co^{II}TpivPP in toluene solution is also sensitive to the environmental conditions as shown in Figure 7. The optical absorption spectrum of tetracoordinated Co(II) porphyrin undergoes only small changes in the Soret peak (404

nm) and in the α peak (563 nm) on forming the pentacoordinated Co(II) porphyrin (Stynes et al., 1973). The optical absorption spectrum of tetracoordinated Co^{II}TpivPP in toluene solution looks like that of pentacoordinated Co^{II}TpivPP·2-methylimidazole. Thus, a possible model of the photodissociated state for species I of oxy–CoMb is that photolysis not only may break the bond between the bound dioxygen and the metal but also may break the bond between the metal and the proximal histidine to form a tetracoordinated low-spin Co(II) complex. This possibility was first considered by Yonetani et al. (1974b) but was not further elaborated. The EPR signal at $g = 2.33$, indicative of the deoxy form, is observable in photolyzed oxy–CoMb below pH 5, which may suggest that the bond between the metal and the proximal histidine in the photolyzed product (species I) is labile. The g values of the photolyzed products were different between oxy–Co-mesoMb and oxy–Co-protoMb. Our recent single-crystal EPR study indicates a difference in the orientation of the bound ligand between oxy–Co-protoMb and oxy–Co-mesoMb (Hori et al., 1982). The difference in the g values between photolyzed forms of oxy–Co-mesoMb and oxy–Co-protoMb may be due to the different orientations of the bound oxygen between them. In the previous spectra of the photolyzed product of oxy–CoMb, the maximal g value was $g = 3.87$ (Yonetani et al., 1974b), whereas it was determined to be $g = 3.55$ in the present experiment. Although the origin of these differences is not apparent at the moment, the photolyzed product (species I) may be unstable, and may be easily affected by details of the protein structure.

In the absence of a base in the axial position, cobalt(II) porphyrins are in an unfavorable situation for magnetic exchange with the dioxygen molecule. Although one cannot exclude the possible formation of the peroxo binuclear cobalt complex, the EPR spectrum of the pentacoordinated dioxygen complex has an EPR absorption near $g \sim 2$, as previously reported (Walker, 1974). The optical absorption spectrum of pentacoordinated oxy–Co^{II}TpivPP, in toluene solution at 77 K, is similar to that of pentacoordinated Co^{II}TpivPP·2-methylimidazole. Thus, another possible model of the photodissociated state for species II in oxy–CoMb is that photolysis may break only the bond between the metal and the proximal histidine, but the bond between the bound dioxygen and the metal still remains the same for species II. The equivalence of deoxy–CoMb to the phtolyzed oxy–CoMb (species I and II) in optical measurements seems to be reasonable from the models of the photodissociated states mentioned above. In Figure 8, the interaction of oxygen with CoMb is schematically presented, based on the analogy of the optical and EPR spectra of cobalt porphyrin model complexes. The absence of hyperfine coupling in the EPR spectra cannot be explained at present. We cannot exclude the possibility that the electronic state is a high-spin Co(II) ion ($S = {}^3/_2$) (Yonetani et al., 1974b). Low-temperature magnetic susceptibility measurement is planned to assign the spin states of the photolyzed product, although the existence of two species (I and II) and of the remaining unphotolyzed oxy–CoMb would make a quantitative analysis difficult.

Photolysis of Nitric Oxide–Cobalt Complexes. The optical absorption spectra of nitric oxide–CoMb and nitric oxide–CoHb (*Glycera*) are changed to the deoxy form upon illumination at 4.2 K. One may expect that the stereochemistry of Co(II) porphyrin in these photolyzed products is similar to that of the photolyzed products of oxy–CoMb and oxy–CoHb (*Glycera*). The loss of the EPR signals of CoMb and CoHb upon reaction with nitric oxide has been interpreted as

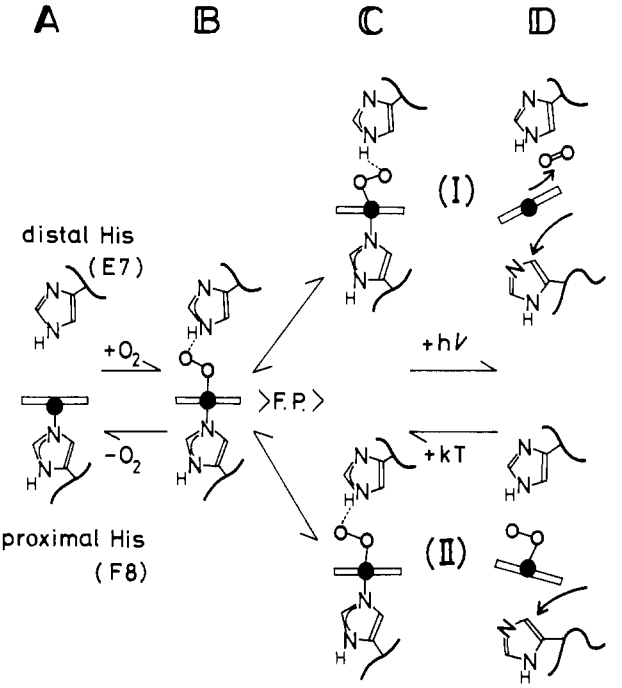

FIGURE 8: Schematic presentation of the interaction of oxygen with CoMb: (A) deoxy–CoMb; (B) oxy–CoMb at ambient temperature; (C) oxy–CoMb at cryogenic temperature (species I and II); (D) photolyzed oxy–CoMb (species I and II). F.P. means the temperature of the freezing point of CoMb, ~−5 °C in solution and ~−35 °C in single-crystal conditions. The solid circle denotes the cobaltous ion, and the open rectangle denotes the porphyrin plane. The dotted line between the liganded oxygen atom and the NH proton of the distal histidine (E7) indicates the possible hydrogen bonding. Arrows in (D) indicate the possible movements of the proximal histidine (F8) and/or the oxygen molecule. (I) and (II) indicate species I and species II.

a spin pairing between the metal and the ligand nitric oxide (Yonetani et al., 1972). New EPR signals could be found in photolyzed products of nitric oxide–CoMb and –CoHb (*Glycera*). As shown in Figure 5B, the photolyzed product of nitric oxide–CoHb (*Glycera*) exhibited a broad EPR signal around $g = 2.33$. When the EPR spectrum of the photolyzed product of oxy–CoHb (*Glycera*) is compared with that of nitric oxide–CoHb (*Glycera*), one puzzle remains. The photodissociated oxygen molecule is paramagnetic, as is nitric oxide, but we cannot observe any magnetic interaction between the Co(II) ion and the dissociated oxygen molecule. The observed line broadening in the photolyzed product of nitric oxide–CoHb (*Glycera*) may be due to magnetic dipole–dipole and exchange interactions between deoxy–CoHb (*Glycera*) ($S = {}^1/_2$) and dissociated nitric oxide ($S = {}^1/_2$). The dipole–dipole interaction depends strongly on the distance (r) between and orientation of the two dipoles. From the line shape of the line-width broadening, of the order β/r^3 where β is Bohr magneton, the average distance between the Co(II) ion and the dissociated nitric oxide is estimated to be ~4 Å (Abragam & Bleaney, 1970). The dissociated nitric oxide molecule may be trapped in the "heme pocket" about 4 Å away from the cobalt ion. As shown in Figure 5A, the EPR spectrum of the photolyzed product of nitric oxide–CoMb, on the other hand, exhibits two signals: one is a broader signal around $g = 2$, and the other is at $g = 4.3$. The EPR signal which appeared at $g = 4.3$ is not readily saturated with microwave power, whereas the signal around $g = 2$ is readily saturated, indicating that these EPR signals have a different electronic origins. Although the origin of these two paramagnetic species, which appeared in the photolyzed product of nitric oxide–CoMb, is

not apparent at the moment, the existence of two species should be expected from the results of oxy-CoMb. The mode of interaction betwen the Co(II) ion and the proximal histidine in nitric oxide-CoMb may be different from that in oxy-CoMb. It will be difficult to demonstrate a model of the photolyzed products of nitric oxide-CoMb, because the electronic and stereochemical natures of the unphotolyzed product of this compound are unknown. Therefore, we will only discuss several possible interpretations of these unusual EPR signals which appeared in the photolyzed product of nitric oxide-CoMb. Sinc ethe nitric oxide-Co(II) complex exhibits no EPR signal due to its strongly coupled spin system, it may be possible to consider that the photolysis weakens this spin-coupling system, and thus, these new EPR signals appear. A broader signal around $g = 2$ indicates that the distance between nitric oxide and Co(II) ion is less than 4 Å. With regard to another EPR signal at $g = 4.3$, the g tensor is nearly isotropic from the single-crystal results. The effective g value, $g = 4.28$, with large hyperfine coupling, has been reported for the high-spin Co(II) complex (Abragam & Bleaney, 1970). However, no hyperfine coupling due tot he ^{59}Co nucleus is observed in our photolyzed product. We failed to observe these photolyzed products of nitric oxide-CoMb with S- and Q-band EPR because of the low intensity of the EPR signal and of the low sensitivity of the EPR equipment. In any case, we cannot exclude the possible interaction between the dissociated nitric oxide and Co(II) ion. This new EPR signal at $g = 4.3$ is though to arise from the weakly coupled system described as exchange interaction between nitric oxide ($S = {}^1/_2$) and Co(II) ion, in which it is unknown whether the spin state is high spin ($S = {}^3/_2$) or low spin ($S = {}^1/_2$). In addition to the EPR signals shown in Figure 4, we have observed another broad EPR signal with low intensity near zero magnetic field in the photolyzed product of nitric oxide-CoMb. Similar EPR signals were also observed in the photolyzed products of nitric oxide-Fe^{3+}Mb and nitric oxide-Mn^{2+}Mb, respectively (unpublished results). These broad EPR signals are considered to arise from the dissociated nitric oxide spin trapped in the heme pocket of the myoglobin molecule.

Mössbauer spectra of the photolyzed products of ligated Fe^{2+}Mb and Fe^{2+}Hb (human) have been reported to be somewhat different from those for their deoxy compounds (Spartalian et al., 1976). Further low-temperature EPR (<4.2 K), ENDOR, and emission Mössbauer measurements will be required in order to facilitate the further theoretical interpretation of the photolyzed forms. We believe that steric interactions of the distal residues as well as the proximal residues would contribute significantly toward the stereochemistry and the electronic state of the metal-ligand bond. Therefore, these interactions should be incorporated in the theoretical analyses of the stereochemistry and in the electronic state of the photolyzed product.

Acknowledgments

We thank Dr. T. Iizuka for discussions and J. M. Palumbo for assistance.

References

Abragam, A., & Bleaney, B. (1970) *Electron Paramagnetic Resonance of Transition Ions*, Clarendon Press, Oxford.

Chacko, V. P., & Manoharan, P. T. (1974) *J. Magn. Reson. 16*, 75–81.

Chien, J. C. W., & Dickinson, L. C. (1972) *Proc. Natl. Acad. Sci. U.S.A. 69*, 2783–2787.

Collman, J. P., Gane, R. R., Reed, C. A., Halbert, T. R., Lang, G., & Robinson, W. T. (1975) *J. Am. Chem. Soc. 97*, 1427–1439.

Collman, J. P., Brauman, J. I., Doxsee, K. M., Harbert, T. R., & Suslik, K. S. (1978) *Proc. Natl. Acad. Sci. U.S.A. 75*, 564–568.

Dickinson, L. C., & Chien, J. C. W. (1982) *Proc. Natl. Acad. Sci. U.S.A. 77*, 1235–1239.

Fantucci, P., & Valenti, V. (1976) *J. Am. Chem. Soc. 98*, 3832–3838.

Goodman, B. A., & Raynor, J. B. (1970) *Adv. Inorg. Chem. Radiochem. 13*, 135–362.

Hoffman, B. M., & Petering, D. H. (1970) *Proc. Natl. Acad. Sci. U.S.A. 67*, 637–643.

Hoffman, B. M., Baslo, F., & Diemente, D. L. (1973) *J. Am. Chem. Soc. 95*, 6497–6498.

Hori, H., Ikeda-Saito, M., & Yonetani, T. (1980) *Nature (London) 288*, 501–502.

Hori, H., Ikeda-Saito, M., & Yonetani, T. (1982) *J. Biol. Chem.* (in press).

Iizuka, T., Yamamoto, H., Kotani, M., & Yonetani, T. (1974) *Biochim. Biophys. Acta 351*, 182–195.

Ikeda-Saito, M., Iizuka, T., Yamamoto, H., Kayne, F. J., & Yonetani, T. (1977) *J. Biol. Chem. 252*, 4882–4887.

Kendrew, J. C., & Parrish, R. G. (1956) *Proc. R. Soc. London, Ser. A 238*, 305–324.

Padlan, E. A., & Love, W. E. (1974) *J. Biol. Chem. 249*, 4067–4078.

Petsko, G. A., Rose, D., Tsernoglou, D., Ikeda-Saito, M., & Yonetani, T. (1978) in *Frontiers of Biological Energetics* (Dutton, P. L., Scarpa, T., & Leigh, J. S., Eds.) pp 1011–1016, Academic Press, New York.

Schonland, D. S. (1959) *Proc. Phys. Soc., London 73*, 788–792.

Spartalian, K., Lung, G., & Yonetani, T. (1976) *Biochim. Biophys. Acta 428*, 281–290.

Stynes, D. V., Stynes, H. C., James, B. R., & Ibers, J. A. (1973) *J. Am. Chem. Soc. 95*, 1796–1801.

Urbach, F. L., Bereman, R. D., Topich, J. A., Hariharan, M., & Kalbacher, B. J. (1974) *J. Am. Chem. Soc. 96*, 5063–5069.

Walker, F. A. (1970) *J. Am. Chem. Soc. 92*, 4235–4244.

Walker, F. A. (1974) *J. Magn. Reson. 15*, 201–218.

Yonetani, T., Yamamoto, H., Erman, J., Leigh, J. S., Jr., & Reed, G. H. (1972) *J. Biol. Chem. 247*, 2447–2455.

Yonetani, T., Yamamoto, H., & Woodrow, G. V. (1974a) *J. Biol. Chem. 249*, 682–690.

Yonetani, T., Yamamoto, H., & Iizuka, T. (1974b) *J. Biol. Chem. 249*, 2168–2174.